MUTATION IN BRIEF

HUMAN MUTATION

A Homozygous *SCN5A* Mutation in a Severe, Recessive Type of Cardiac Conduction Disease

Axel Neu[1,2], Michele Eiselt[3], Matthias Paul[4], Kathrin Sauter[1], Birgit Stallmeyer[5,6], Dirk Isbrandt[1], and Eric Schulze-Bahr[4-6]

[1] Experimental Neuropediatrics, [2] Department of Pediatrics, [3] Department of Pediatric Cardiology, University Medical Center Hamburg-Eppendorf, Germany; [4] Department of Cardiology and Angiology, [5] Genetics of Heart Diseases, [6] Interdisciplinary Clinical Research Center (IZKF), University Hospital Münster, Germany

Correspondence to: Univ.-Prof. Dr. Eric Schulze-Bahr, Schwerpunkt Genetik von Herzerkrankungen, Universitätsklinikum Münster, D-48129 Münster, E-mail: Eric.Schulze-Bahr@ukmuenster.de

Communicated by Garry R. Cutting

ABSTRACT: Cardiac sodium channels are key players in the generation and propagation of action potentials in the human heart. Heterozygous mutations in the *SCN5A* gene have been found to be associated with long QT syndrome, Brugada syndrome, and sinus node dysfunction (SND). Recently, overlapping arrhythmia phenotypes have been reported as well. Here we describe a novel recessive *SCN5A* mutation in a family originating from the German minority in White Russia. Four affected children with a history of early cardiac arrhythmia encompassing SND, conduction disease, and severe ventricular arrhythmias, are homozygous carriers of a novel *SCN5A* missense mutation (p.I230T) in the channel protein. Interestingly, the heterozygous mutation carriers had neither significant ECG abnormalities nor a history of cardiac events. Heterologous expression of SCN5A(I230T) channels revealed normal protein transport but altered biophysical sodium channel properties. Voltage range of both activation and inactivation were shifted in a way that resulted in decreased sodium current and loss of channel function. In conclusion, we describe a rare clinical condition with a novel *SCN5A* mutation causing a new type of complex cardiac arrhythmia. Unlike most previously reported sodium channelopathies, this overlap syndrome displays recessive inheritance characteristics and does not seem to follow simple Mendelian rules. ©2010 Wiley-Liss, Inc.

KEY WORDS: SCN5A; cardiac ion channel; arrhythmia; conduction disease

Received 29 January 2010; accepted revised manuscript 25 May 2010.

DOI:10.1002/humu.21302

INTRODUCTION

Cardiac arrhythmias in the absence of structural abnormalities are a growing group of hereditary disorders. Both familial and sporadic cases are associated with mutations in ion channel subunits causing altered ion flux across the plasma membrane (Marban, 2002). The clinical phenotypes such as sinus node dysfunction (SND), conduction block, or disturbances of myocellular repolarization (e.g., long or short QT syndromes) are often life threatening and therefore a major cause of cardiac pacemaker implantation in young patients (Morita et al., 2008).

Voltage-gated sodium channels mediate large sodium currents that completely activate and inactivate within milliseconds (George, 2005). They play a key role in controlling the fast upstroke of the cardiac action potential in both the conduction system and working myocardium. In addition, cardiac sodium channels seem to be involved in slow pacemaker depolarization in the sinus node (Lei et al., 2005; Lei et al., 2007), and an association between loss of sodium channel function and atrial non-excitability (the so-called atrial stand still) has been reported (Benson et al., 2003). The major (alpha) subunit of the cardiac sodium channel is encoded by the *SCN5A* gene on chromosome 3p21 (MIM# 600163). Mutations in the *SCN5A* gene and also in auxiliary SCN5A subunits have been found in a broad spectrum of familial and sporadic arrhythmias (Bennett et al., 1995; Chen et al., 1998; Schott et al., 1999; Wang et al., 1995; Watanabe et al., 2008).

With regard to the functional effects on the resulting net sodium current, *SCN5A* mutations can generally be subdivided into two groups. Gain-of-function mutations in the *SCN5A* gene are typically associated with congenital long QT syndrome (LQTS) of subtype 3, resulting in an increase of sodium currents by slow or incomplete channel inactivation (Bennett et al., 1995; George, 2005; Wang et al., 1995). In contrast, loss-of-function mutations reduce net sodium currents either by impairing channel trafficking or by shifting voltage dependence of activation and inactivation. These mutations are associated with a broader and overlapping spectrum of supraventricular and ventricular arrhythmias including atrial stand still, Brugada syndrome, and cardiac conduction disease (Benson et al., 2003; Chen et al., 1998; Rook et al., 1999; Tan et al., 2001; Wang et al., 2002). In addition, distinct mutations in *SCN5A* may be linked to even more complex cardiac arrhythmias with overlapping phenotypes due to a combination of loss and gain of function (Makita et al., 2008; Smits et al., 2005; Surber et al., 2008; Tan et al., 2007). However, it is still not completely understood how the respective mutations cause the resulting clinical phenotype, which is likely to be modified by intrafamilial and individual variability in myocardial conductance and repolarization.

In the present study, we describe a family with four children presenting with a severe and complex phenotype of cardiac arrhythmia. Screening of the *SCN5A* gene resulted in the detection of a novel, homozygous *SCN5A* mutation c.689T>C in all four affected children. To study the mechanisms determining the malignant phenotype, we analyzed subcellular transport and biophysical properties of mutated SCN5A channel proteins in HEK293 cells.

MATERIALS AND METHODS

Clinical evaluation

Clinical data of both parental family lines were collected from 22 available members of a family that belongs to the ethnic German minority in White Russia (now living in Germany). Based on a genealogical reconstruction using church books, it was possible to trace both parental family lines back to two geographical areas in White Russia that were only about 50 km apart, making the possibility of consanguinity more likely. Individual clinical data, including age at diagnosis, gender, family history of sudden cardiac death, and specific cardiac symptoms (syncope, cardiac arrest, tachycardia) were collected. For all genotyped individuals, at least one standard 12-lead ECG recording was performed when the individual was off medication.

In addition, an intravenous ajmaline test was performed in three individuals who were identified to be carriers of one mutant *SCN5A* allele (including both parents of the severely affected children, IDs 2, 3, and 16; Fig. 1C; final ajmaline dosage: 1 mg/kg body weight at an injection rate of about 10 mg/min) to screen for the presence of latent Brugada syndrome. Seven family members (all affected children, IDs 1, 5-7, and IDs 2, 3, and 16; Fig. 2D) were examined for structural heart disease using transthoracic echocardiography.

Definitions and normal ECG values: For heart rate (HR), the lower range was defined by 90 bpm (under 2 years of age), 60 bpm (6-13 years of age) and 50 bpm (adults), (Rautaharju et al., 1979). The upper values for normal

atrioventricular conduction (PQ interval) were 150 ms (HR 90-110/min) and 130 ms (HR 130-150/min) (both values refer to individuals under 2 years of age), 160 ms (2-13 years of age), and 200 ms (adults). For the QRS interval, the upper normal values were 30-70 ms (under 2 years of age), 40-90 ms (2-13 years of age), and 110 ms (adults). Brugada syndrome was diagnosed according to the current criteria: presence of the so-called type 1 ECG (in more than one ECG lead) that is defined as a prominent coved ST segment elevation displaying J wave amplitude or ST segment elevation $\geq$2 mm (or 0.2 mV) at its peak followed by a negative T wave, either under baseline conditions or after ajmaline challenge (Antzelevitch et al., 2005; Wilde et al., 2002).

Molecular genetics

Genomic DNA was extracted from whole blood, and the cardiac sodium channel gene *SCN5A* (GenBank accession number M77235.1) was completely sequenced as described before (Schulze-Bahr et al., 2003). Nucleotide numbering reflects cDNA numbering with +1 corresponding to the A of the ATG translation initiation codon in the reference sequence. PCR primer sequences and amplification conditions for the highly polymorphic markers D3S3727 - D3S3518 - D3S3623 – [*SCN5A*] - D3S3521 - D3S3597 - D3S1568 (deCODE map position interval: 55.39 – 59.21 - 62.73 – [63.72] - 64.35 - 68.38 - 70.89 cM) on chromosome 3p24-p21 were obtained from the NCBI database. Two-point logarithm of the odds (LOD) scores was calculated with the MLINK program 5.1 (http://www.cs.uiowa.edu/ ~jni/glas/). To determine the location score on chromosome 3p by multipoint analysis, we performed SIMWALK2.91 analysis. Using an autosomal recessive disease model as obvious from the pedigree (Fig. 2D), penetrance was set to 1.0, and for the disease frequency a value of 0.00001 was assumed.

All subjects had given written informed consent after counseling. The study was in accordance with the ethical standards of the Declaration of Helsinki (2001) and with recommendations given by the Ethics Committee of the University of Münster. All DNA-identified variants were compared with a control group of more than 380 unrelated, healthy individuals from the Caucasian population.

Generation of stable cell lines

Full-length wild-type SCN5A cDNA (GenBank accession number M77235.1) was cloned into the pcDNA5-FRT vector (Invitrogen), and the point mutation c.689T>C was introduced by site-directed mutagenesis and verified by direct sequencing. Subsequently, stable cell lines expressing either SCN5A wild-type (WT) or SCN5A(I230T) were established using the HEK flip-in system (Invitrogen).

For electrophysiological recordings, cells were seeded on 35 mm dishes, transfected with 3.5 µg lipofectamine (Invitrogen) and 1.5 µg plasmid DNA containing the cardiac sodium channel ß1 subunit (SCN1B) and eGFP and were used for recordings 4-5 days after transfection.

Western blot and immunocytochemistry

For Western blot, cells were rinsed twice with ice-cold PBS, incubated for 1.5 h in 250 µl lysis buffer (50 mM Hepes pH 7.4, 150 mM NaCl, 0.5% Triton-X100, 2.5 µl proteinase inhibitor mix (Sigma), and centrifuged at 10,000 g for 10 min. The supernatant (19 µl) was separated under reducing conditions by SDS page using NuPage 8-12% gradient gels (Invitrogen). Subsequently, proteins were transferred onto Protran nitrocellulose membranes. Membranes were blocked for 1 h in blocking solution (5% non-fat dry milk powder in PBS, 0.05% Tween-20) before adding anti-SCN5A polyclonal antibodies (rabbit, Chemicon) diluted 1:500 in antibody solution (1% non-fat dry milk powder in PBS, 0.05% Tween-20). After incubation for 1 h at room temperature, membranes were washed in PBS, 0.05% Tween-20), followed by incubation with peroxidase-labeled anti-rabbit IgG (1:5000, Vector). Lava purple staining was used afterwards to control for equal overall protein content.

For immunocytochemistry, HEK293 cells were seeded on poly-L-lysine-coated cover slips and transfected with 2 µl Turbofect (Fermentas) and 1 µg plasmid DNA containing a C-terminally truncated CD4 that was efficiently transported to the surface (Zerangue et al., 2001). 24 h after transfection and before permeabilization, cells were incubated in a medium containing 1% goat serum, 0.2% BSA, 0.1% Trition-X100 and monoclonal CD4 antibodies (RPA-T4, mouse, 1:500, eBioscience) in PBS for 1h. Cells were then fixed with 4% paraformaldehyde in PBS for 20min. After blocking for 1 h in a medium containing 10% goat serum, 0.2% BSA, 0.1% Trition-X100 in PBS, immunostaining was performed in 1% goat serum, 0.2% BSA, 0.1% Trition-X100 in PBS with an anti-SCN5A polyclonal antibody (rabbit, 1:500; Chemicon). Alexa 488-labeled anti-mouse IgG (1:1000; Molecular Probes) and Alexa 555-labeled anti-rabbit IgG (1:500; Molecular Probes) were used as secondary antibodies. Cover slips were

mounted with DAPI-Fluoromount (SouthernBiotech) to stain nuclei. Confocal images were analyzed using a laser scanning microscope (Fluoview 100, Olympus).

Cellular electrophysiology

Sodium currents were recorded using the outside-out patch-clamp technique (Hamill et al., 1981). Currents were acquired at 20 kHz using an EPC9 amplifier and PULSE+PULSE FIT software (HEKA). All experiments were performed at 20-22°C. The bath solution contained (in mM):145 NaCl, 4 KCl, 1.8 $CaCl_2$, 1 $MgCl_2$, 10 HEPES, and 10 glucose, pH 7.35 (adjusted with NaOH). The pipette solution contained (in mM): 10 NaF, 110 CsF, 20 CsCl, 10 EGTA, and 10 HEPES, pH 7.35 (adjusted with CsOH). The time between sequential test protocols was 10 s, and the holding potential was –120 mV for all experiments. For current densities, current amplitudes were divided by the membrane area calculated from the electrode tip size. The P4 method was used to subtract leak and capacitive currents from raw traces. Only stable patches with leak currents <50 pA were used.

Excel (Microsoft) and Igor Pro (WaveMetrics) were used for data analysis and statistics. To determine voltage dependence of activation and inactivation, maximal sodium currents were divided by the electrochemical driving force according to the Nernst equation and fitted with the Boltzmann function $G = a / (1+\exp((V_{1/2} - V) /k))$, where a is the maximal conductance, $V_{1/2}$ is the half-maximal activation, and k the slope factor. Both the time course of inactivation and the time course of recovery from inactivation were fit with two-exponential functions. All data are given as mean ± SEM. Statistical significance ($p<0.05$) was assessed with Student's t test.

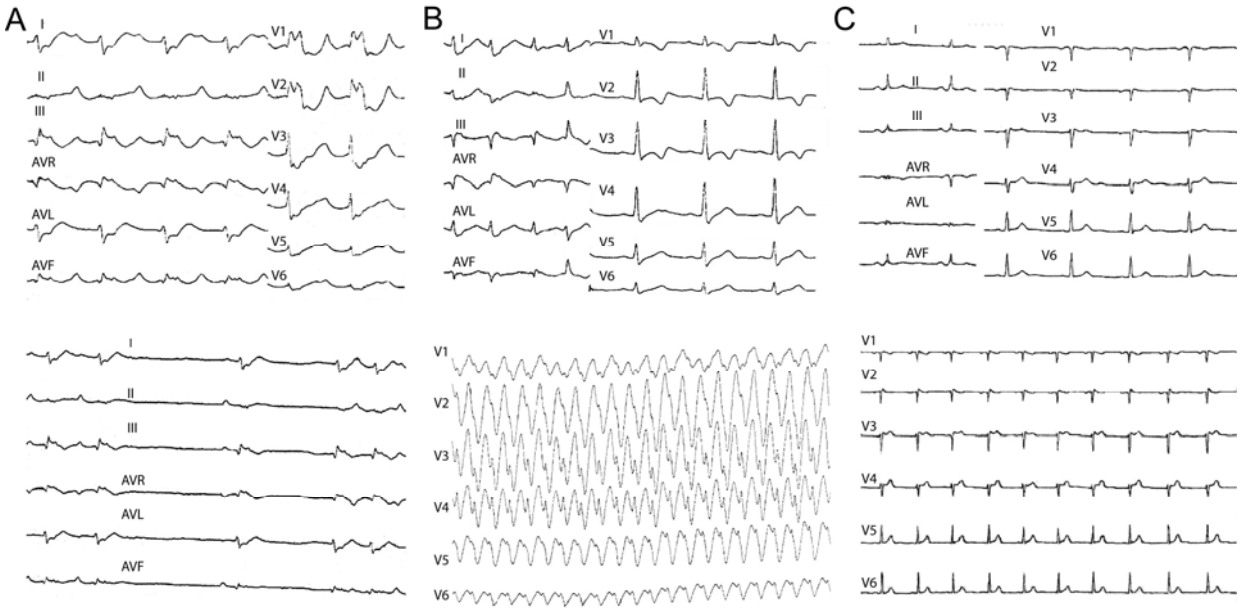

Figure 1. (**A**) ECG of the index patient (ID 1) at 6 years of age. The patient had Ebstein's anomaly, progressive heart failure, and bradycardia. Top: 12-lead ECGs showed an unusual right bundle branch block (200 ms) and right axis deviation, absence of an isoelectric ST segment due to inhomogeneous depolarization, and secondary repolarization disturbances (QT 490 ms). In addition, first-degree AV conduction block with prominent and prolonged P waves (due to Ebstein's anomaly) and right ventricular hypertrophy. Bottom: Sinus bradycardia due to non-excitability of the atria (either due to sinus node arrest or atrial inexcitability). (**B**) Top: a 12-lead ECG of the index patients sister (ID 6) at 1.25 years of age shows AV block of 1st degree (150 ms), right bundle branch block (100 ms, prolonged for age), and left axis deviation. Bottom: Monomorphic ventricular tachycardia (188 bpm) during an episode of fever. (**C**) ECG of the father (ID 2) who was heterozygous carrier of the *SCN5A* c.689C allele at 34 years of age. In the upper ECG, rSR' morphology in leads V1-V3, only in V3 significant J point elevation (1.5 mm), and saddle-back (type III Brugada) ECG. No evident/diagnostic type I ECG for Brugada syndrome or conduction abnormality. In the ECG recorded after full dose of ajmaline (bottom), J-point elevation in V3 and V4 and a saddle-back ST segment as well as an upright T wave were seen. No signs of Brugada syndrome.

RESULTS

Clinical evaluation

A 6-year-old boy (ID 1) was admitted to the hospital because of dyspnea and cyanosis. His previous medical history was unremarkable except for bacterial meningitis at the age of 3 years. The baseline ECG, however, showed clear signs of severe cardiac conduction disease in terms of complete right bundle branch block and prolonged AV conduction (Fig. 1A). In addition, transthoracic echocardiography revealed Ebstein's anomaly, second-degree tricuspid valve insufficiency, and non-compaction-like cardiomyopathy. Screening for metabolic, infectious, or immunologic causes of left ventricular dilatation remained negative, and a cardiac biopsy showed only unspecific histologic changes. Due to chronotropic incompetence and declining left ventricular function, the patient underwent dual-chamber pacemaker implantation and received carvedilol and, following documented ventricular tachycardia, amiodarone. Despite optimized therapy for heart failure, left heart function decreased progressively, requiring biventricular pacing and, finally, extracorporeal membrane oxygenation and biventricular assist device implantation. However, the patient died at the age of 12 years due to progressive heart failure and fatal ventricular fibrillation prior to highly urgent heart transplantation.

Mutation detection in the *SCN5A* gene

The clinical phenotype consisting of an overlap of a severe atrial and ventricular conduction system disorder and the occurrence of ventricular arrhythmia during an episode of fever prompted us to screen for mutations in the cardiac sodium channel gene *SCN5A*. As a result, a homozygous nucleic acid substitution (c.689T>C, exon 6) was detected in the index patient (ID 1) and, later on, in all three siblings (ID 5-7) (Fig. 2A). At the amino acid level, the point mutation is predicted to result in a non-synonymous substitution of the hydrophobic amino acid isoleucine for the more hydrophilic amino acid threonine at position 230 (p.I230T)(Fig. 2B). Absence of the *SCN5A* c.689C allele in a large number of control samples (380 unrelated Caucasians) suggests that it is not a rare polymorphism. Note the conservation of the isoleucine residue at position 230 of the SCN5A protein across species (Fig. 2C).

Next, we investigated other family members from a large pedigree of 22 available members spanning at least three generations (Fig. 2D). As expected, both asymptomatic parents (ID 2 and 3) were heterozygous carriers of the *SCN5A* c.689C allele, as were ten other asymptomatic family members (a total of 11 are shown in Fig. 2D). The remaining asymptomatic individuals did not carry the mutant allele. In summary, we identified four homozygous and 12 heterozygous mutation carriers for *SCN5A* c.689C.

To determine whether there was a common origin of the mutant *SCN5A* c.689C allele, we subsequently used six microsatellite markers at both sites of the *SCN5A* gene for investigation of a common haplotype. Using the highly polymorphic markers D3S3727 - D3S3518 - D3S3623 – [*SCN5A*] - D3S3521 - D3S3597 - D3S1568 on chromosome 3p24-p21, we not only showed homozygosity for the *SCN5A* mutation, but also for all fragment lengths of each marker in the four siblings (IDs 1, 5-7). In addition, we were able to trace the fragment lengths back to the generations available for the study, and consistently found that all other heterozygous mutation carriers had a common chromosome 3 fragment that ranged from D3S3727 (map position 55.39 cM) to D3S3597 (68.38 cM) and encompassed *SCN5A,* suggesting a common origin of mutant alleles (Fig. 2D). Haplotypes and two-point LOD scores for all markers finally revealed significant linkage with a LOD score of 3.86 (with *SCN5A* locus) at a recombination fraction θ of 0 (MLINK 5.1 analysis, Table 1).

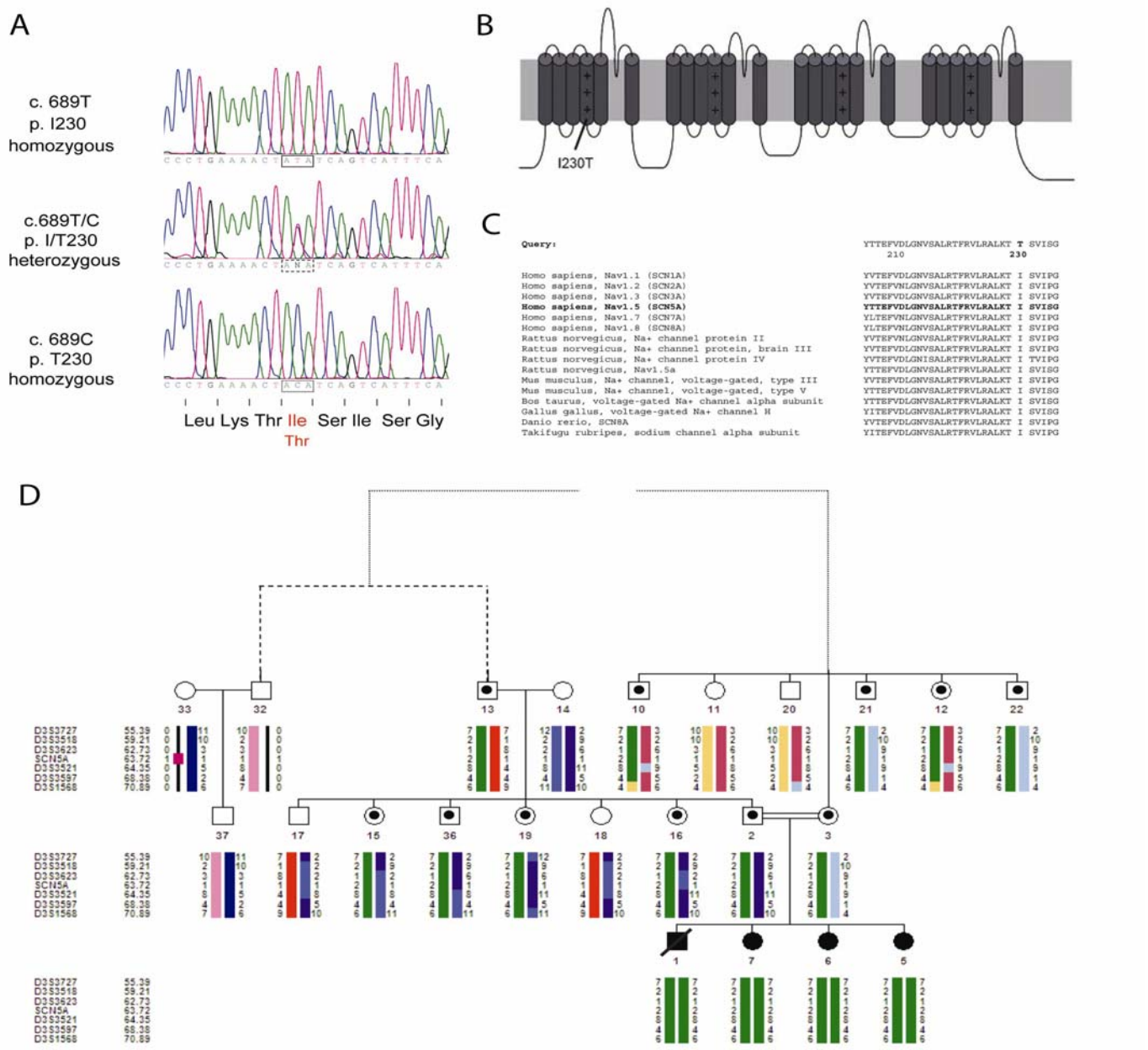

Figure 2. (**A**) Electropherogram after direct sequencing of a wild-type control (top panel), the index patient (ID 1, bottom panel), and his mother (ID 3, middle panel). A homozygous nucleic acid substitution (c.689T>C) was detected in exon 6 of the index patient's *SCN5A* gene, while heterozygosity for this alteration was detected in the *SCN5A* gene of the index patient's mother. (**B**) Schematic topology of SCN5A channels with intracellular N- and C-termini and 4 domains with six transmembrane segments each. The point mutation c.689T>C is predicted to result in a single amino acid substitution p.I230T in the voltage-sensing segment of the first channel domain (arrow). Relative size of transmembrane segments and extra- and intracellular linkers are not drawn to scale. (**C**) Alignment of the protein domain around the altered amino acid residue 230 showed a high degree of conservation when compared with related sodium channel proteins or orthologs of SCN5A. **(D)** Pedigree of the large White Russian family (family ID: 10458). Males are shown as squares, females as circles. Points indicate heterozygous carrier status, whereas filled symbols mark homozygous individuals. All affected children (IDs 1, 5-7) were homozygous for the mutation, whereas both parents (IDs 2, 3) were heterozygous for *SCNA* c.689T>C. Microsatellite analysis with flanking markers at each site of *SCN5A* (centromer: D3S3727 - D3S3518 - D3S3623 – *SCN5A* - D3S3521 - D3S3597 - D3S1568) on chromosome 3p24-p21 revealed an identical fragment between markers D3S3727 (deCODE map position interval: 55.39 cM) and D3S3597 (64.35 cM) coinherited with the mutant *SCN5A* c.689C allele. Note: Recombination between markers D3S3597 and D3S1568 in individuals 10 and 12, respectively. LOD score calculations are given in Table 1.

Clinical and ECG data of mutation carriers

Given the dramatic and fatal clinical course of the index patient (ID 1), the family has been systematically evaluated, including targeted mutation detection through double-strand DNA sequencing. Surprisingly, all three sisters of the index patient were also identified as homozygous mutation carriers. They were first diagnosed with SND at routine examinations. The four homozygous *SCN5A* mutation carriers had an ECG at 3.6 (±2.5) years of age. With regard to age, all four subjects had sinus bradycardia with a first-degree AV block and significantly prolonged age-corrected QRS intervals (135±53 ms). One girl (ID 7) was additionally diagnosed with recurrent ventricular tachyarrhythmia at the age of 4 years. Following pacemaker implantation, sotalol treatment was started, and no further clinical complications occurred. Another sister (ID 6) had right bundle block and recurrent ventricular tachyarrhythmia during episodes of fever (Fig. 1B). She, too, underwent pacemaker implantation and remained clinically stable while receiving sotalol treatment. Despite obvious SND and conduction disease, the youngest girl (ID 5) has not yet shown any clinical symptoms, and has developed normally without any treatment to date. Consanguinity of the parents (IDs 2 and 3) was not reported, but they originated from neighboring villages in White Russia. Both parents were healthy and never experienced symptomatic arrhythmia or syncope in the past. Routine ECGs were normal, without signs of SND, conduction disorder, or ventricular arrhythmia. There was no history of cardiac events in any of the remaining 16 asymptomatic family members available for clinical examination. Using the genetic test, we identified a total of 12 heterozygous mutation carriers including both parents. The PQ interval was prolonged in 50% (mean PQ interval: 197±28 ms), but none of them had QRS prolongation (mean: 83±7 ms), abnormal QRS axis deviation, or sinus bradycardia (HR: 70.4±2.8 bpm). Taken together, in 50% of 12 heterozygous mutation carriers, who were all clinically asymptomatic, an AV block of 1° was present.

Because the affected children's phenotypes were reminiscent of overlap syndromes caused by *SCN5A* mutations, both parents and the mother's sister (IDs 2, 3 and 16) were challenged with ajmaline to test for the presence of latent Brugada syndrome (Wilde et al., 2002). However, no ECG alterations typical of Brugada syndrome, such as ST elevation or right bundle branch block, were observed in any of the tested individuals (ECG of the father: Fig. 1C). There was no evidence of structural heart disease or abnormal cardiac function in the three female homozygous *SCN5A* mutation carriers and four other heterozygous mutation carriers (including both parents) as demonstrated by transthoracic echocardiography (not shown).

Table 1. LOD score report after two-point analysis using MLINK 5

Order	0.0	0.01	0.05	0.1	0.2
D3S3727	2.92	2.86	2.62	2.31	1.71
D3S3518	1.54	1.49	1.29	1.06	0.71
D3S3623	3.15	3.09	2.84	2.52	1.89
SCN5A	**3.86**	**3.79**	3.53	3.18	2.45
D3S3521	2.52	2.46	2.24	1.96	1.42
D3S3597	3.19	3.13	2.89	2.59	1.97
D3S1568	2.25	2.19	1.98	1.73	1.23

Intracellular trafficking of wild-type and mutant SCN5A channels

To determine the pathomechanisms underlying the arrhythmic phenotype, we generated stable cell lines expressing SCN5A(WT) or SCN5A(I230T). Both cell lines expressed comparable steady-state amounts of SCN5A protein detected by Western blot analysis (Fig. 3A). Subcellular location and trafficking of SCN5A(I230T) channels was analyzed with an antibody against the intracellular linker between the first two homologous channel domains (DI-DII). Similar immunostaining patterns and intensities were obtained for cells expressing either wild-type or mutant SCN5A protein (Fig. 3B). In both cases, channels were not only located in the plasma membrane, but also to a large extent around the nucleus, indicating high protein turnover in the stable cell lines. Therefore, impaired intracellular SCN5A(I230T) channel trafficking (a so-called class 2 mutation mechanism) was not a likely cause of the observed cardiac phenotype.

Biophysical characterization of SCN5A(I230T)

Interestingly, the mutation is located in the fourth transmembrane domain known to be involved in voltage-dependent gating of sodium channels (Fig. 2B). As protein synthesis and channel trafficking were normal, we subsequently analyzed the biophysical properties of SCN5A(WT) and SCN5A(I230T) sodium channels. To minimize voltage error and series resistance and to control membrane size, sodium currents were recorded in the outside-out patch-clamp configuration (Hamill et al., 1981). Both SCN5A(WT) and SCN5A(I230T) channels gave rise to typical inward currents that completely inactivated within milliseconds (Fig. 4A). However, SCN5A(I230T) currents activated at more depolarized potentials (–60 mV, n=16 vs. -70 mV for WT, n=16), and showed significantly smaller current densities (122±20 pA/µm^2, n=16 vs. 297±62 pA/µm^2 for WT, n=16; p= 0.015) than SCN5A(WT) currents (Fig. 4B). We performed additional experiments to determine the mechanisms responsible for sodium current reduction in mutant channels. As shown in Fig. 4C, the midpoint of activation of SCN5A(I230T) channels was significantly shifted about 15 mV to more positive potentials compared to SCN5A(WT) channels (–35.5±1.7 mV, n= 11; vs. –50.9±1.7 mV for WT, n= 12; p< 0.01). In contrast, steady-state availability showed a minor shift of about 5 mV to more negative potentials (–90.9±1.4 mV for WT, n= 9; vs. –95.8±1.9 mV, n= 13; p= 0.047) (Fig. 4C). Other kinetic channel parameters (e.g., time constants of inactivation and recovery from inactivation) were unchanged (Fig. 4D, 4E).

Our biophysical analyses demonstrate that the sodium current reduction observed in SCN5A(I230T) channels can be explained by a positive shift in activation, accompanied by a negative shift in inactivation compared to SCN5A(WT) channels. This so-called class 3 mechanism in conjunction with the genetic data make the pathogenic nature of SCN5A(I230T) highly likely.

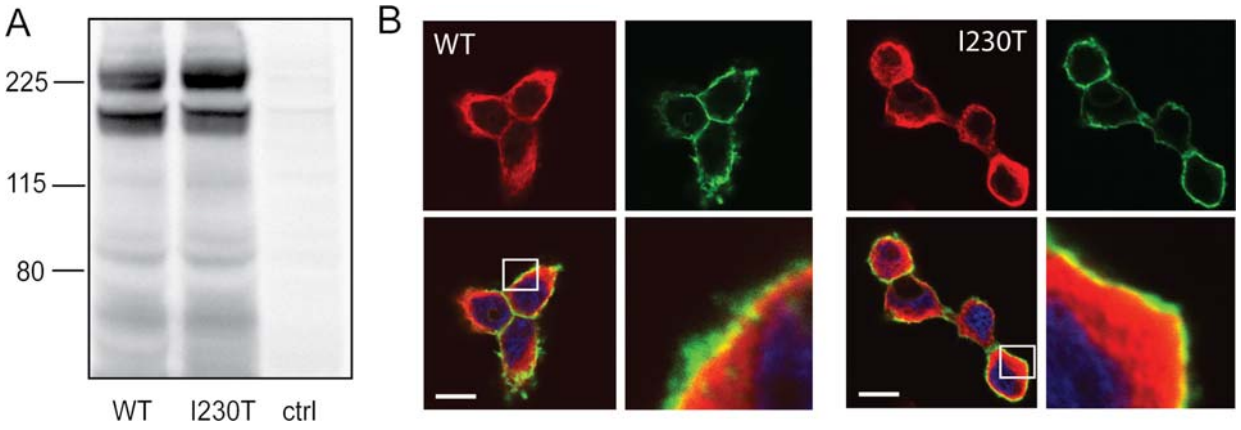

Figure 3. (**A**) Western blot analysis demonstrates comparable amounts of SCN5A channel protein in WT and I230T expressing cell lines. (**B**) Similar distributions of SCN5A(WT) (left) and SCN5A(I230T) (right) proteins with immunoreactivities detectable in perinuclear regions and at the plasma membrane (red). For membrane staining, cells were transfected with CD4 and stained before permeabilization (green). Nuclei were stained by DAPI (blue). Note the partial overlap of SCN5A and CD4 staining (yellow, bottom). Scale bar 10µm. White frames indicate magnified areas (bottom left).

DISCUSSION

Loss-of-function mutations in the genes encoding subunits for the cardiac sodium channel are typically associated with a broad spectrum of cardiac arrhythmia disturbances that predominantly include cardiac conduction disease, Brugada syndrome, SND, and atrial stand still (Priori, 2009). In line with these findings, several studies have shown an association of *SCN5A* mutations with overlap syndromes including atrial and ventricular arrhythmia (Remme et al., 2008). The majority of reported sodium channel gene mutations are heterozygous in state. Recessively inherited mutations are exceptionally rare (Benson et al., 2003; Frigo et al., 2007; Lupoglazoff et al., 2001), and are expected to show a gene dosage effect. In the present study, we identified a novel, homozygous missense mutation in the cardiac *SCN5A* gene leading to a severe clinical phenotype in four

children, including SND, ventricular tachyarrhythmia, conduction block, and congenital heart disease in at least one child. Apart from these four homozygous mutation carriers, 12 heterozygous mutation carriers showed no significant ECG abnormalities, even after pharmacological challenge with ajmaline (n=3 individuals). Taken together, *SCN5A* c.689T>C showed typical genetic features of a recessive inheritance pattern and, unexpectedly, a preferential transmission of the mutated *SCN5A* allele.

Genetics

In our study, all affected individuals are homozygous carriers of the c.689C allele and share a common haplotype on chromosome 3p21. Although there was no known relationship between family members of previous generations of both parental family lines, a common ancestor carrying the founder mutation is likely, particularly in view of the relatively isolated German community in White Russia and the proximity of the villages of origin. The pathogenic nature of this novel mutation is supported by several findings: a) we established genetic linkage between microsatellite markers at the *SCN5A* locus and the disease phenotype; b) only individuals homozygous for the disease haplotype were symptomatic, supporting the notion that *SCN5A* c.689T>C is indeed a pathogenic mutation; c) *SCN5A* c.689T>C was not detected in samples from a large control group, therefore ruling out a typical polymorphism; d) the I230 residue is highly conserved across different species; and e), the disease relevance of the mutation was supported by electrophysiological analysis of the resulting channel protein demonstrating significant sodium current reduction in the presence of normal channel trafficking.

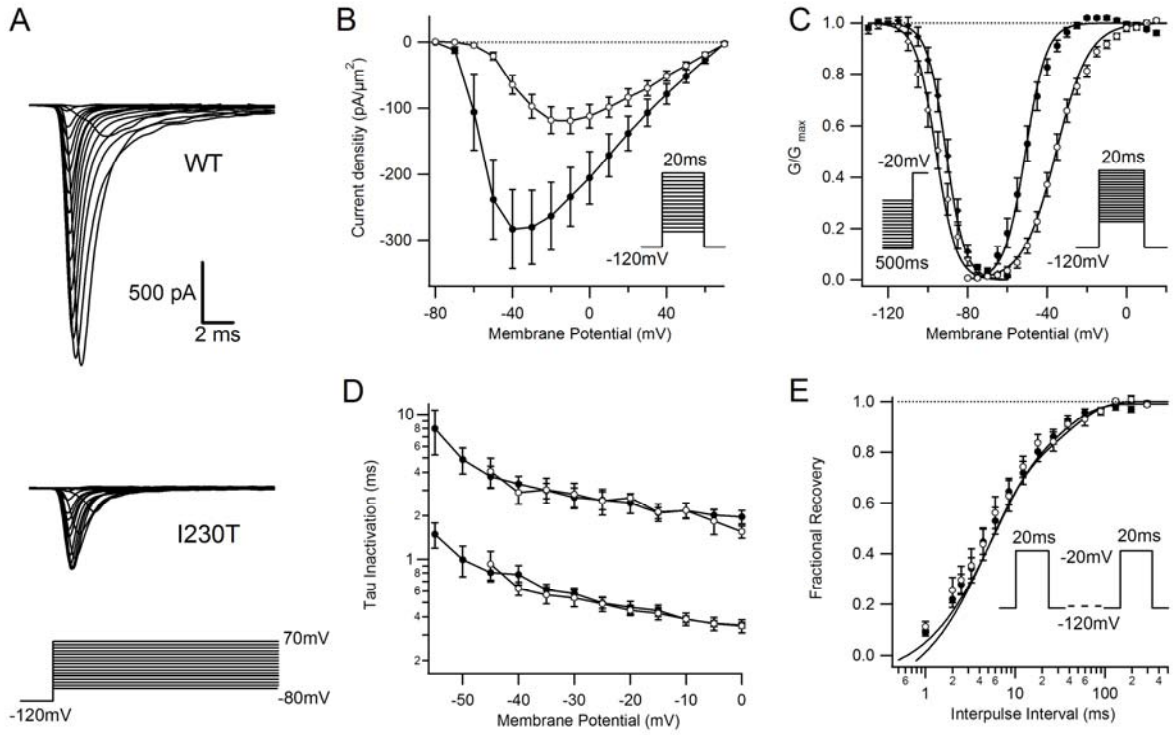

Figure 4. (A) Example current traces of SCN5A(WT) and SCN5A(I230T) channels from stable cell lines following depolarizing voltage steps from –80 mV to +70 mV in 10 mV steps. (**B**) Current densities of SCN5A(WT) (filled circles) and SCN5A(I230T) (open circles) in excised patches. (**C**) Voltage dependence of activation and steady-state inactivation of SCN5A(WT) (filled circles) and SCN5A(I230T) (open circles) channels. (**D**) Time constants of fast and slow inactivation of SCN5A(WT) (filled circles) and SCN5A(I230T) (open circles) channels. (**E**) Recovery from inactivation of SCN5A(WT) (filled circles) and SCN5A(I230T) (open circles) channels.

In *SCN5A*-associated channelopathies, dominant modes of inheritance underpinning the importance of two fully functional *SCN5A* copies were found (Remme et al., 2006). However, there are only few reports in which recessive

traits with asymptomatic heterozygous mutation carriers were identified (Benson et al., 2003; Bezzina et al., 2003; Lupoglazoff et al., 2001). In our study, the homozygous mutation carriers were the only family members who presented with clinical symptoms and showed full penetrance. Apart from PQ-prolongation, heterozygous mutation carriers displayed normal cardiac function, without signs of arrhythmia or conduction disorder, even under ajmaline challenge, which supports the assumption of a recessive mode of inheritance. The lack of a clinical phenotype in heterozygous individuals might be attributed to unknown compensatory effects (e.g., functionally relevant polymorphisms in other cardiac ion channels) that partially counteract the loss of sodium inward currents (Groenewegen et al., 2003), or to an overall minor effect of the mutant allele in the presence of one functional wild-type copy. Alternatively, accessory but yet unknown sodium channel subunits could potentially be upregulated, thereby shifting back the voltage dependence of SCN5A(I230T) channels toward physiological ranges *in vivo*. Finally, it has to be taken into account that previous studies did not show clear phenotype-genotype correlations in SCN5A channelopathies, although the absence of a clinical phenotype in heterozygous mutation carriers is not likely given the significant current reduction caused by SCN5A(I230T).

A puzzling observation in our study is that the complete offspring of the last generation were homozygous for the disease-causing mutation *SCN5A* c.689T>C. Based on the assumption of simple Mendelian inheritance, the probability of homozygosity for four independent combinations would be less than 0.4%. Furthermore, 71% instead of the expected 50% of the offspring of the previous generation were heterozygous mutation carriers. Given the relatively small number of individuals, this trait is still compatible with Mendelian inheritance, but additional factors favoring transmission of the *SCN5A* c.689C allele might exist. For example, the presence of additional pathogenic ion channel mutations that are partially compensated by reduced sodium conductance might explain the preferential inheritance of the *SCN5A* c.689C allele. In this context, it is interesting to note that an unequal transmission ratio has recently been described for mutations in cardiac potassium channels (Imboden et al., 2006). However, we believe this preferential and concomitant transmission of both mutant *SCN5A* alleles to be a singular, extraordinary event.

Clinical and pathophysiologic aspects

All affected patients in our study displayed SND and, except for one subject (ID 5), ventricular tachyarrhythmia requiring pacemaker implantation. Interestingly, the only affected boy (ID 1) had the most severe phenotype, including extreme conduction block and Ebstein's anomaly with heart failure. We therefore wondered whether the broad spectrum of disorders in this single patient might be exclusively explained by sodium channel dysfunction, or whether additional genetic and acquired factors contributed to the phenotype. Apart from Ebstein's anomaly, no additional metabolic or infectious factors causing this inborn cardiac defect were identified, not even by *post-mortem* tissue analysis (data not shown). Furthermore, there is distinct evidence of a causative role for the *SCN5A* gene in structural heart disease and hereditary cardiomyopathy (Frigo et al., 2007; McNair et al., 2004; Olson et al., 2005; Shi et al., 2008). However, structural or histopathologic abnormalities in patients with *SCN5A* mutations are not a common finding (Zumhagen et al., 2009), and in accordance with the variability in ECG presentation, not all homozygous *SCN5A* mutation carriers had evident congenital heart disease. In addition to the ongoing discussion on the contribution of sodium channel gene mutations to structural heart disease, there is increasing evidence from reports showing their involvement in atrial fibrillation and heart failure (Darbar et al., 2008). Among the potential disease-modifying factors, gender differences leading to more severe phenotypes in males have frequently been recognized in Brugada syndrome (Eckardt, 2007; Matsuo et al., 2003) and in specialized clinical practice (Schulze-Bahr, unpublished). Although other influencing factors in addition to sodium channel dysfunction cannot be ruled out, the patient's severe phenotype clearly represents a summation of almost all *SCN5A*-related cardiac disorders.

Previously detected mutations associated with SCN5A overlap syndromes mainly resulted in a loss of sodium channel function, as analyzed in heterologous expression systems (Remme et al., 2008). Accordingly, sodium currents evoked by SCN5A(I230T) channels were reduced to about 45% of control levels. In general, reduced ion flux can be caused by a decreased number of channels or altered gating properties. There was no indication of a reduced number of channels in the plasma membrane due to altered SCN5A(I230T) protein trafficking, making a class 2 mutation effect unlikely. As the missense mutation resulted in a substitution of the hydrophobic amino acid isoleucine for the polar amino acid threonine in a voltage sensor, reduced single channel conductance was highly unlikely. Indeed, in our study, the combination of a positive shift of voltage dependence of activation and a negative shift of voltage dependence of inactivation was sufficient to explain the current reduction.

Interestingly, a mutation encoding an isoleucine to valine substitution at the same position (I230V) was found in a patient with Brugada syndrome (Schulze-Bahr et al., 2003). This conservative amino acid substitution might underlie the milder clinical phenotype of this case as compared to that of malignant arrhythmia observed in our present study.

In view of the complex dysfunction in rhythm generation and propagation in affected individuals, the detailed mechanism causing the clinical phenotype remains elusive. Computational modeling studies are undertaken to investigate arrhythmias affecting mostly restricted myocardial subpopulations, such as isolated SND or LQTS. In several studies, the generation of SND, Brugada syndrome, and LQTS was analyzed by entering biophysical properties of mutated cardiac sodium channels into well-established computer models of sinus node, conduction system, or myocardial cells (Clancy and Rudy, 2002). Unfortunately, there is no comprehensive model that includes all relevant myocardial regions affected in our patients. Therefore, we can only speculate that the moderate sodium current reduction in heterozygous mutation carriers is too mild to disrupt physiological rhythm generation, but that the loss of more than 50% of SCN5A–mediated sodium currents cannot be compensated for in homozygous individuals.

In summary, we provide evidence for a novel point mutation in the voltage sensor of the major cardiac sodium channel gene *SCN5A* causing a complex phenotype of early-onset arrhythmia in homozygous mutation carriers due to reduced sodium currents. Our findings extend the spectrum of SCN5A channelopathies to include an overlap phenotype consisting of cardiac arrhythmia, cardiomyopathy and also potentially congenital structural heart disease.

AKNOWLEDGMENTS

We gratefully acknowledge the excellent assistance of El. Schulze-Bahr, M. Raetz, M. Keuthen, and A. Nigmann. We thank A. Zeisser and S. Schillemeit for help with cell culture, and A. Isbrandt for comments on the manuscript. We are indebted to the patients and individuals who participated in the present study.

The work was supported by grants from the Deutsche Forschungsgemeinschaft (Schu 1082/3-1 and /3-2, IS63/1–1/2), the Interdisciplinary Center for Clinical Research (IZKF) of the University of Münster, Germany, and by the Fondation Leducq, Paris, France.

REFERENCES

Antzelevitch C, Brugada P, Borggrefe M, Brugada J, Brugada R, Corrado D, Gussak I, LeMarec H, Nademanee K, Perez Riera AR and others. 2005. Brugada syndrome: report of the second consensus conference: endorsed by the Heart Rhythm Society and the European Heart Rhythm Association. Circulation 111:659-70.

Bennett PB, Yazawa K, Makita N, George AL, Jr. 1995. Molecular mechanism for an inherited cardiac arrhythmia. Nature 376:683-5.

Benson DW, Wang DW, Dyment M, Knilans TK, Fish FA, Strieper MJ, Rhodes TH, George AL, Jr. 2003. Congenital sick sinus syndrome caused by recessive mutations in the cardiac sodium channel gene (SCN5A). J Clin Invest 112:1019-28.

Bezzina CR, Rook MB, Groenewegen WA, Herfst LJ, van der Wal AC, Lam J, Jongsma HJ, Wilde AA, Mannens MM. 2003. Compound heterozygosity for mutations (W156X and R225W) in SCN5A associated with severe cardiac conduction disturbances and degenerative changes in the conduction system. Circ Res 92:159-68.

Chen Q, Kirsch GE, Zhang D, Brugada R, Brugada J, Brugada P, Potenza D, Moya A, Borggrefe M, Breithardt G and others. 1998. Genetic basis and molecular mechanism for idiopathic ventricular fibrillation. Nature 392:293-6.

Clancy CE, Rudy Y. 2002. Na(+) channel mutation that causes both Brugada and long-QT syndrome phenotypes: a simulation study of mechanism. Circulation 105:1208-13.

Darbar D, Kannankeril PJ, Donahue BS, Kucera G, Stubblefield T, Haines JL, George AL, Jr., Roden DM. 2008. Cardiac sodium channel (SCN5A) variants associated with atrial fibrillation. Circulation 117:1927-35.

Eckardt L. 2007. Gender differences in Brugada syndrome. J Cardiovasc Electrophysiol 18:422-4.

Frigo G, Rampazzo A, Bauce B, Pilichou K, Beffagna G, Danieli GA, Nava A, Martini B. 2007. Homozygous SCN5A mutation in Brugada syndrome with monomorphic ventricular tachycardia and structural heart abnormalities. Europace 9:391-7.

George AL, Jr. 2005. Inherited disorders of voltage-gated sodium channels. J Clin Invest 115:1990-9.

Groenewegen WA, Firouzi M, Bezzina CR, Vliex S, van Langen IM, Sandkuijl L, Smits JP, Hulsbeek M, Rook MB, Jongsma HJ and others. 2003. A cardiac sodium channel mutation cosegregates with a rare connexin40 genotype in familial atrial standstill. Circ Res 92:14-22.

Hamill OP, Marty A, Neher E, Sakmann B, Sigworth FJ. 1981. Improved patch-clamp techniques for high-resolution current recording from cells and cell-free membrane patches. Pflugers Arch 391:85-100.

Imboden M, Swan H, Denjoy I, Van Langen IM, Latinen-Forsblom PJ, Napolitano C, Fressart V, Breithardt G, Berthet M, Priori S and others. 2006. Female predominance and transmission distortion in the long-QT syndrome. N Engl J Med 355:2744-51.

Lei M, Goddard C, Liu J, Leoni AL, Royer A, Fung SS, Xiao G, Ma A, Zhang H, Charpentier F and others. 2005. Sinus node dysfunction following targeted disruption of the murine cardiac sodium channel gene Scn5a. J Physiol 567:387-400.

Lei M, Zhang H, Grace AA, Huang CL. 2007. SCN5A and sinoatrial node pacemaker function. Cardiovasc Res 74:356-65.

Lupoglazoff JM, Cheav T, Baroudi G, Berthet M, Denjoy I, Cauchemez B, Extramiana F, Chahine M, Guicheney P. 2001. Homozygous SCN5A mutation in long-QT syndrome with functional two-to-one atrioventricular block. Circ Res 89:E16-21.

Makita N, Behr E, Shimizu W, Horie M, Sunami A, Crotti L, Schulze-Bahr E, Fukuhara S, Mochizuki N, Makiyama T and others. 2008. The E1784K mutation in SCN5A is associated with mixed clinical phenotype of type 3 long QT syndrome. J Clin Invest 118:2219-29.

Marban E. 2002. Cardiac channelopathies. Nature 415:213-8.

Matsuo K, Akahoshi M, Seto S, Yano K. 2003. Disappearance of the Brugada-type electrocardiogram after surgical castration: a role for testosterone and an explanation for the male preponderance. Pacing Clin Electrophysiol 26:1551-3.

McNair WP, Ku L, Taylor MR, Fain PR, Dao D, Wolfel E, Mestroni L. 2004. SCN5A mutation associated with dilated cardiomyopathy, conduction disorder, and arrhythmia. Circulation 110:2163-7.

Morita H, Wu J, Zipes DP. 2008. The QT syndromes: long and short. Lancet 372:750-63.

Olson TM, Michels VV, Ballew JD, Reyna SP, Karst ML, Herron KJ, Horton SC, Rodeheffer RJ, Anderson JL. 2005. Sodium channel mutations and susceptibility to heart failure and atrial fibrillation. JAMA 293:447-54.

Priori SG. 2009. Arrhythmias: Unexplained sudden cardiac death--back to clinical evaluation. Nat Rev Cardiol 6:678-9.

Rautaharju PM, Davignon A, Soumis F, Boiselle E, Choquette A. 1979. Evolution of QRS-T relationship from birth to adolescence in Frank-lead orthogonal electrocardiograms of 1492 normal children. Circulation 60:196-204.

Remme CA, Verkerk AO, Nuyens D, van Ginneken AC, van Brunschot S, Belterman CN, Wilders R, van Roon MA, Tan HL, Wilde AA and others. 2006. Overlap syndrome of cardiac sodium channel disease in mice carrying the equivalent mutation of human SCN5A-1795insD. Circulation 114:2584-94.

Remme CA, Wilde AA, Bezzina CR. 2008. Cardiac sodium channel overlap syndromes: different faces of SCN5A mutations. Trends Cardiovasc Med 18:78-87.

Rook MB, Bezzina Alshinawi C, Groenewegen WA, van Gelder IC, van Ginneken AC, Jongsma HJ, Mannens MM, Wilde AA. 1999. Human SCN5A gene mutations alter cardiac sodium channel kinetics and are associated with the Brugada syndrome. Cardiovasc Res 44:507-17.

Schott JJ, Alshinawi C, Kyndt F, Probst V, Hoorntje TM, Hulsbeek M, Wilde AA, Escande D, Mannens MM, Le Marec H. 1999. Cardiac conduction defects associate with mutations in SCN5A. Nat Genet 23:20-1.

Schulze-Bahr E, Eckardt L, Breithardt G, Seidl K, Wichter T, Wolpert C, Borggrefe M, Haverkamp W. 2003. Sodium channel gene (SCN5A) mutations in 44 index patients with Brugada syndrome: different incidences in familial and sporadic disease. Hum Mutat 21:651-2.

Shi R, Zhang Y, Yang C, Huang C, Zhou X, Qiang H, Grace AA, Huang CL, Ma A. 2008. The cardiac sodium channel mutation delQKP 1507-1509 is associated with the expanding phenotypic spectrum of LQT3, conduction disorder, dilated cardiomyopathy, and high incidence of youth sudden death. Europace 10:1329-35.

Smits JP, Koopmann TT, Wilders R, Veldkamp MW, Opthof T, Bhuiyan ZA, Mannens MM, Balser JR, Tan HL, Bezzina CR and others. 2005. A mutation in the human cardiac sodium channel (E161K) contributes to sick sinus syndrome, conduction disease and Brugada syndrome in two families. J Mol Cell Cardiol 38:969-81.

Surber R, Hensellek S, Prochnau D, Werner GS, Benndorf K, Figulla HR, Zimmer T. 2008. Combination of cardiac conduction disease and long QT syndrome caused by mutation T1620K in the cardiac sodium channel. Cardiovasc Res 77:740-8.

Tan BH, Iturralde-Torres P, Medeiros-Domingo A, Nava S, Tester DJ, Valdivia CR, Tusie-Luna T, Ackerman MJ, Makielski JC. 2007. A novel C-terminal truncation SCN5A mutation from a patient with sick sinus syndrome, conduction disorder and ventricular tachycardia. Cardiovasc Res 76:409-17.

Tan HL, Bink-Boelkens MT, Bezzina CR, Viswanathan PC, Beaufort-Krol GC, van Tintelen PJ, van den Berg MP, Wilde AA, Balser JR. 2001. A sodium-channel mutation causes isolated cardiac conduction disease. Nature 409:1043-7.

Wang DW, Viswanathan PC, Balser JR, George AL, Jr., Benson DW. 2002. Clinical, genetic, and biophysical characterization of SCN5A mutations associated with atrioventricular conduction block. Circulation 105:341-6.

Wang Q, Shen J, Splawski I, Atkinson D, Li Z, Robinson JL, Moss AJ, Towbin JA, Keating MT. 1995. SCN5A mutations associated with an inherited cardiac arrhythmia, long QT syndrome. Cell 80:805-11.

Watanabe H, Koopmann TT, Le Scouarnec S, Yang T, Ingram CR, Schott JJ, Demolombe S, Probst V, Anselme F, Escande D and others. 2008. Sodium channel beta1 subunit mutations associated with Brugada syndrome and cardiac conduction disease in humans. J Clin Invest 118:2260-8.

Wilde AA, Antzelevitch C, Borggrefe M, Brugada J, Brugada R, Brugada P, Corrado D, Hauer RN, Kass RS, Nademanee K and others. 2002. Proposed diagnostic criteria for the Brugada syndrome: consensus report. Circulation 106:2514-9.

Zerangue N, Malan MJ, Fried SR, Dazin PF, Jan YN, Jan LY, Schwappach B. 2001. Analysis of endoplasmic reticulum trafficking signals by combinatorial screening in mammalian cells. Proceedings of the National Academy of Sciences of the United States of America 98:2431-6.

Zumhagen S, Spieker T, Rolinck J, Baba HA, Breithardt G, Bocker W, Eckardt L, Paul M, Wichter T, Schulze-Bahr E. 2009. Absence of pathognomonic or inflammatory patterns in cardiac biopsies from patients with Brugada syndrome. Circ Arrhythm Electrophysiol 2:16-23.